



Controls on the development and persistence of soil moisture drought across Southwestern Germany

Erik Tijdeman and Lucas Menzel

Institute of Geography, Professorship in Hydrology and Climatology, Heidelberg University, Heidelberg, Germany

5

Correspondence to: Erik Tijdeman (erik.tijdeman@uni-heidelberg.de)

Abstract

The drought of 2018 in Central and Northern Europe showed once more the large impact this natural hazard can have on the environment and society. Such droughts are often seen as slowly developing phenomena. However, root zone soil moisture
10 deficits can rapidly develop during periods of lacking precipitation and meteorological conditions that favour high evapotranspiration rates. These periods of soil moisture drought stress can persist for as long as the meteorological drought conditions last, thereby negatively affecting vegetation and crop health. In this study, we aim to characterize past soil moisture drought stress events over the cropland of South-Western Germany as well as to relate the characteristics of these
15 past events to different soil and climate properties. We first simulated daily soil moisture over the period 1989-2018 on a 1-km resolution grid using the physical based hydrological model TRAIN. We then derived various soil moisture drought stress characteristics; likelihood, development time and persistence, from the simulated time series of all agricultural grid cells ($n \approx 15000$). Logistic regression and correlation were then applied to relate the derived characteristics to the storage capacity of the root zone as well as to the climatological setting. Results reveal that the majority of the agricultural grid cells across the study region reached soil moisture drought stress during prominent drought years. The development time of these
20 soil moisture drought stress events varied substantially, from as little as 10 days to up to 4 months. The persistence of soil moisture drought stress varied as well and was especially high for the drought of 2018. The dominant control on the likelihood and development time of soil moisture drought stress was found to be the storage capacity of the root zone, whereas the persistence was not strongly linearly related to any of the considered controls. Overall, results give insights in the large spatial and temporal variability of soil moisture drought stress characteristics and highlight the importance of
25 considering differences in root zone soil storage for agricultural drought assessments.

1 Introduction

Droughts are naturally (re-)occurring phenomena that can appear in different domains of the hydrological cycle and cause associated impacts (Tallaksen and Van Lanen 2004; Stahl et al., 2016). Because of their multifaceted characteristics, droughts are often classified in different types (Wilhite & Glantz, 1985). One of these drought types is agricultural drought,



30 which refers to the impacts of lacking water availability on the health and growth of crops. These agricultural droughts can
reduce yields and thereby cause large economic losses. A crucial first step to reduce the risk of (agricultural) drought impacts
involves effective monitoring and early warning of the drought hazard (UN/ISDR, 2009). Agricultural drought monitoring
and early warning occurs at different scales; from plot-scale observations and simulations to regional-scale drought mapping.
Regional-scale drought monitoring and early warning provides an aerial overview of regions at drought risk, which raises
35 awareness and helps decision-making. Accurately depicting areas affected by agricultural drought is complex as its
occurrence is influenced by a variety of factors, including often spatially heterogeneous climate and soil characteristics. A
better understanding how these climate and soil characteristics control (the development of) agricultural droughts is needed.
Droughts are often defined as a below normal water availability (Tallaksen and Van Lanen 2004). This definition of drought
forms the basis of many drought indices, which reflect whether a certain hydro-meteorological variable is anomalously low
40 or high (e.g., Lloyd-Hughes, 2014). Soil moisture anomaly time series, or proxies of the latter, are often used for agricultural
drought assessments (e.g., Sheffield et al. , 2004; Andreadis et al., 2005; Samaniego, et al., 2012). Different drought
characteristics can be derived from these soil moisture anomaly time series, including drought magnitude, duration, and areal
extent.

The data used for agricultural drought assessments stems from different sources. These data sources include direct soil
45 moisture measurements, remote sensing observations, meteorological proxies and hydrological- or land surface model
simulations (e.g., Berg and Sheffield, 2018). Soil moisture measurements provide the most realistic information about the
soil moisture status at a certain depth but are point based and thereby limited in their spatial coverage. Remote sensing
observations can provide a regional coverage but are only able to detect soil moisture changes in the upper soil layer, at least
in the case of microwave remote sensing. Meteorological proxies for agricultural drought include drought indices such as the
50 Palmer Drought Severity Index (PDSI; Palmer, 1965) or the Standardized Precipitation Evapotranspiration Index (SPEI,
Vicente-Serrano et al., 2010). The strength of these meteorological proxies is their relative ease of computation and often
low data requirements. However, meteorological proxies are often based on potential evapotranspiration and do not consider
some other relevant terrestrial processes that influence soil moisture and agricultural drought, such as the reduction of
evapotranspiration during soil moisture drought stress. Many of these terrestrial processes are included in physical-based
55 hydrological and land surface models. The physical basis of these models makes their use often preferable over the use of
meteorological proxies for past and future agricultural drought assessments (e.g., Berg & Sheffield, 2018; Sheffield et al.,
2012).

Various hydrological and land surface models have been used to assess past and future soil moisture drought events. One
example is the Variable Infiltration Capacity model (VIC), which has been applied to characterize major soil moisture
60 drought episodes across different regions (e.g., US: Sheffield et al., 2004; Andreadis et al., 2005; China: Wang et al., 2011;
and the world: Sheffield & Wood, 2007). The latter analyses enabled the cataloguing of past soil moisture drought events
according to a variety of characteristics, providing a benchmark for current and future drought events. Another example of a
regionally applied model to simulate soil moisture (drought) is the mesoscale Hydrological Model (mHM, Samaniego et al.,



2010). The output of the mHM has been used for both historic soil moisture drought assessments (Hanel et al., 2018) as well
65 as for future soil moisture drought projections across Europe (as part of a model ensemble in Samaniego et al., 2018). The
latter studies provide valuable insights about the severity of recent soil moisture drought events over Europe, e.g., 2003 and
2015, and also show that these recent events were not as rare when considered in a more long-term historical perspective and
that similar or worse events are likely to occur under different climate change scenarios. The mHM is also run in near-real
time and its output is used by the German Drought Monitor (Zink et al., 2016).

70 Studies mentioned in the previous paragraph focus on characterizing past and future soil moisture drought events, whereas
other studies aim to characterize its development. A common consensus about the development of drought is its slowly
nature that can take up to years to reach its full extent (Wilhite & Glantz, 1985). However, not all drought events are slowly
developing phenomena and soil moisture deficits can develop relatively quickly during dry weather conditions that favor
high amounts of evapotranspiration (e.g., Hunt et al. 2009). These rapid developing droughts, sometimes termed “flash
75 droughts”, can severely impact agriculture (e.g., Svoboda et al., 2002, Otkin et al., 2018). Several case-study flash drought
events in the US have been described in Otkin et al. (2013; 2016). The latter studies show that precipitation deficits can be
quickly followed by a reduction of evapotranspiration, which is indicative for low soil moisture levels causing drought stress
for plants. Christian et al. (2019) aimed to make a regional assessment of past flash droughts and developed a framework of
objective criteria to identify flash drought events from simulated soil moisture output. By applying this framework to soil
80 moisture simulations over the US, they show that particular regions, such as the Great Plains, are more sensitive to flash
drought occurrence.

Most of the above-described soil moisture drought assessments characterize drought as a below normal anomaly, which is in
line with the traditional definition of drought. However, from an agricultural drought impact perspective, it might sometimes
make more sense to directly study the characteristics of (the development of) periods of lacking amounts of root zone soil
85 moisture, i.e., soil moisture drought stress, which is in line with the soil moisture drought index proposed in Hunt et al.
(2009). Following this reasoning and inspired by the methods used in previous soil moisture anomaly studies, we aim to
study simulated soil moisture drought stress events across Southwestern Germany. Our objectives are to:

- 1) Characterize past soil moisture drought stress events,
- 90 2) Investigate dominant controls on soil moisture drought stress characteristics
- 3) Portray meteorological anomalies during (the development of) soil moisture drought stress

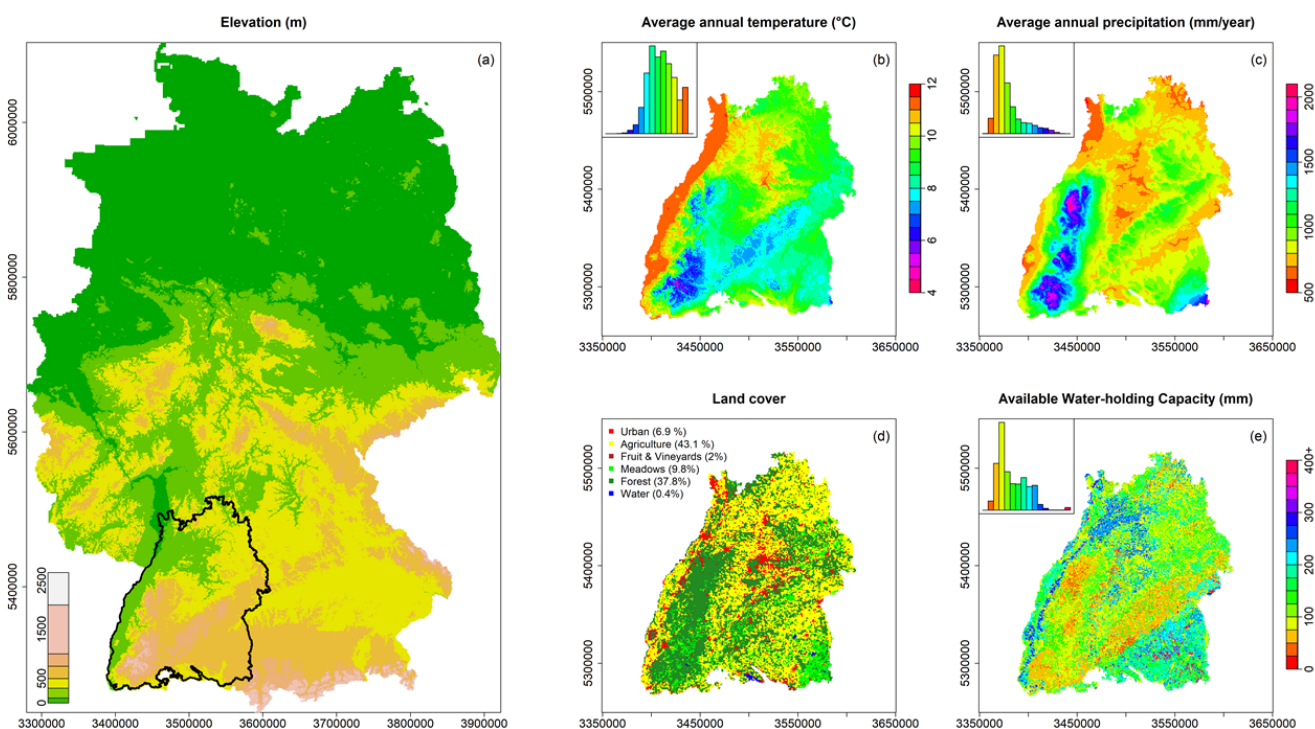
2 Data and methods

2.1 Study region

The study region encompasses Baden-Württemberg (area $\approx 36000\text{km}^2$), a federal state of Germany located in the
95 Southwestern part of the country (Fig. 1). The area of interest covers both flat and lowland regions such as the Rhine valley



as well as higher located, more mountainous regions such as the Black Forest and the Swabian Jura (Fig. 1a). The topography of the study region affects both temperature (annual average between 4.5 °C and 11.6 °C, Fig. 1b) and precipitation (annual average sum between < 600 mm and > 2000 mm, Fig. 1c). Land cover and soil characteristics vary over the study region (Fig. 1d,e). Most of the cropland is located in the lower areas (Fig. 1d). Thicker soils with a higher available water-holding capacity (AWC, i.e., the amount of plant available water in the root zone at field capacity) are generally found in the valleys, and more shallow soils with a lower AWC in the higher elevated, mostly forested regions (Fig. 1d,e).



105 **Figure 1: Study region and its (a) elevation, (b) average annual temperature, (c) average annual precipitation sum, (d) land cover and (e) available water-holding capacity of the root zone soil. Gridded data used to derive this Figure are described in Section 2.2.**

2.2 Data and interpolation

The data used in this study stem from various sources. Gridded elevation data (1-km resolution) were obtained from the Federal Agency for Cartography and Geodesy (BKG, 2018). Vectorized land cover data come from the Corine-2006 dataset and were retrieved from the German Environment Agency (UBA, 2018). Vectorized soil property data (field capacity and wilting point of the root zone soil) were derived from the BK-50 (scale of 1:50,000) dataset provided by the Federal State Office for Geology Resources and Mining (LGRB, 2019). Daily meteorological data for the period between 1989-2018 used in this study stem from both gridded data as well as station-based observations. Gridded precipitation (P, mm) comes from the REGNIE dataset (Rauthe et al., 2013) and was sourced from the climate data center of the German Weather Service



(DWD, 2019). Gridded satellite based global radiation data (RG, watt/m^2) stem from the SARA dataset and were derived
115 from the Satellite Application Facility on Climate Monitoring (Pfeifroth et al., 2019a,b). Station-based meteorological
observations of temperature (T, °C), relative humidity (RH, %) and sunshine duration (SSD, hours) as well as sub-daily
observations of wind speed (U_{speed} , Bft) and wind direction ($U_{\text{direction}}$, °) originate from the climate data center of the German
Weather Service (DWD, 2019). The sub-daily values of U_{speed} and $U_{\text{direction}}$ were aggregated to daily values (for U_{speed} :
arithmetic average, for $U_{\text{direction}}$: average of Cartesian coordinates).
120 All data were interpolated to 1-km resolution grids covering Baden-Württemberg. Land cover and soil property data were
interpolated based on the majority class within each grid cell. Gridded meteorological data were re-projected to match the
extent and resolution of the soil and land cover grids. Station-based meteorological observations were interpolated to grids of
T, U_{speed} , RH and RG using the INTERMET software (Dobler et al. 2004; software ran in default settings). The software first
converts (the units of) some of the meteorological observations, i.e., U_{speed} (Bft) to U_{speed} (m/s) and SSD to RG. The software
125 then interpolates these (and all other) meteorological observations to daily grids using different kriging-based interpolation
techniques. These interpolation techniques consider distance to the station, and, depending on the variable, the possible
relationship between the variable of interest and other external factors such as elevation, wind direction, or relief. The grids
of RG interpolated with INTERMET were only used for days for which the SARA dataset did not provide any data (< 0.25
% of days).

130 2.3 Soil moisture modelling

We applied the physically based hydrological model TRAIN to simulate different fluxes such as evapotranspiration and
percolation as well as the soil moisture status at a daily resolution over Baden-Württemberg. The TRAIN model follows
some basic principles, of which the most important ones are the applicability of the model on both the plot and the areal
scale (e.g., Stork & Menzel, 2016; Törmros & Menzel, 2014) as well as the ability to run the model with as few input data as
135 possible. The latter might reduce the accuracy of the model on the plot scale but benefits its general applicability on larger
scales.

TRAIN includes information from comprehensive field studies of the water and energy balance for different surface types,
including natural vegetation and cropland (Menzel, 1997; Stork & Menzel, 2016). Special focus in the model is on the water
and energy fluxes at the soil-vegetation-atmosphere interface. The simulation of transpiration is based on the Penman-
140 Monteith equation. It depends on the calculation of canopy resistances, which are modified by the state of growth of the
vegetation, soil moisture status and weather conditions (Menzel, 1996). Interception and interception evaporation are
simulated according to Menzel (1997): The maximum amount of water that can be stored in the canopy is dependent on the
seasonal development of the leaf area index LAI. Interception evaporation is modelled to occur with different intensities, as a
function of the actual amount of water accumulated in the canopy and the present weather conditions. The calculation of the
145 soil water status and of percolation follows the conceptual approach from the HBV-model (Bergström, 1995). Thus, the root
zone soil is not subdivided into different layers but understood as one uniform soil column.



The TRAIN model requires hourly or daily information on precipitation, global or net radiation, air temperature, relative humidity and wind speed as input. Information regarding soil depth and its water-holding capacity is also essential to run the model as well as information about the LAI and vegetation/crop height. The latter information can be directly provided to the model or is estimated within the model from typical values, such as the seasonal development of LAI, of specific land use classes.

The TRAIN model was set up with the derived soil and land cover grids and forced with the derived meteorological fields (Section 2.2). Each grid cell was assigned a land cover class as well as an available water-holding capacity (AWC), which was calculated from the difference between field capacity and wilting point of the root zone soil. The initial conditions of root zone soil moisture were set to field capacity at the start of the model run on the first of January of 1988. The first year (1988) was used as warm-up years (only one year to get the initial snow conditions right), whereas the following 30 years (1989-2018) were used for the analyses. Snapshots of the soil moisture status during different stages of the drought year 2018 are shown in Figure 2; complete daily animations of soil moisture status during different drought years are stored in an online repository (Tijdeman and Menzel, submitted together with this article). This online repository also contains all the evaluated daily simulations of soil moisture.

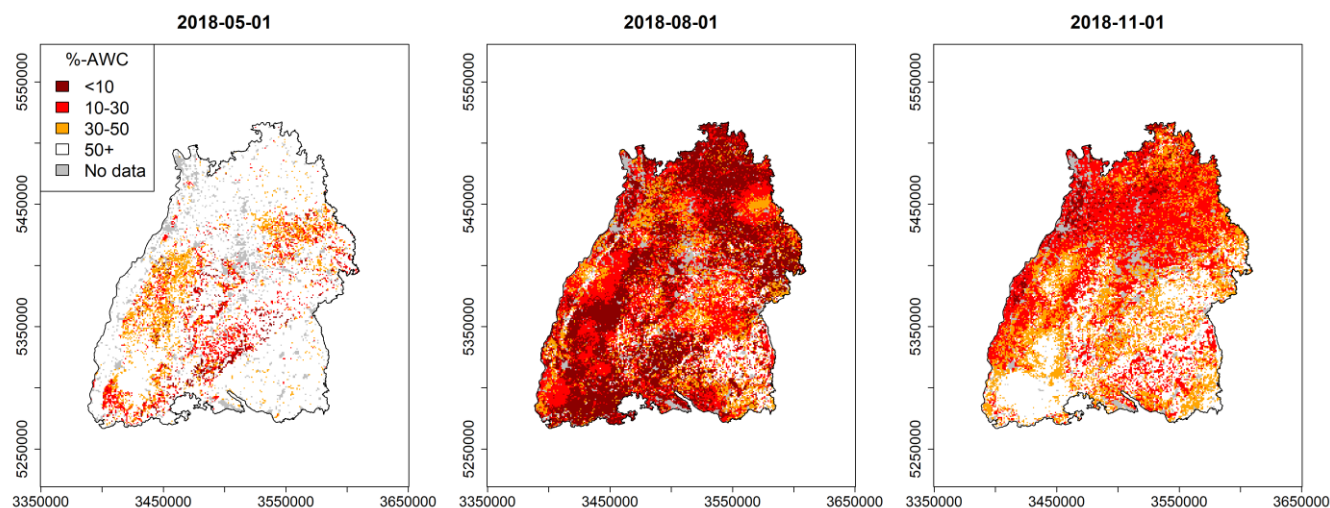


Figure 2. Simulated soil moisture (expressed as the % of AWC left in the root zone) during different stages of the drought of 2018.

In this study, we specifically analyzed simulated soil moisture (SM, expressed as the % of AWC left in the root zone) and simulated total evapotranspiration (E, mm/day). From now on, we focus on grid cells classified as agricultural, as the focus of this study is on agricultural drought. We used a general agricultural land use parameterization, as crop-specific information about which crop was grown where and when was not available.



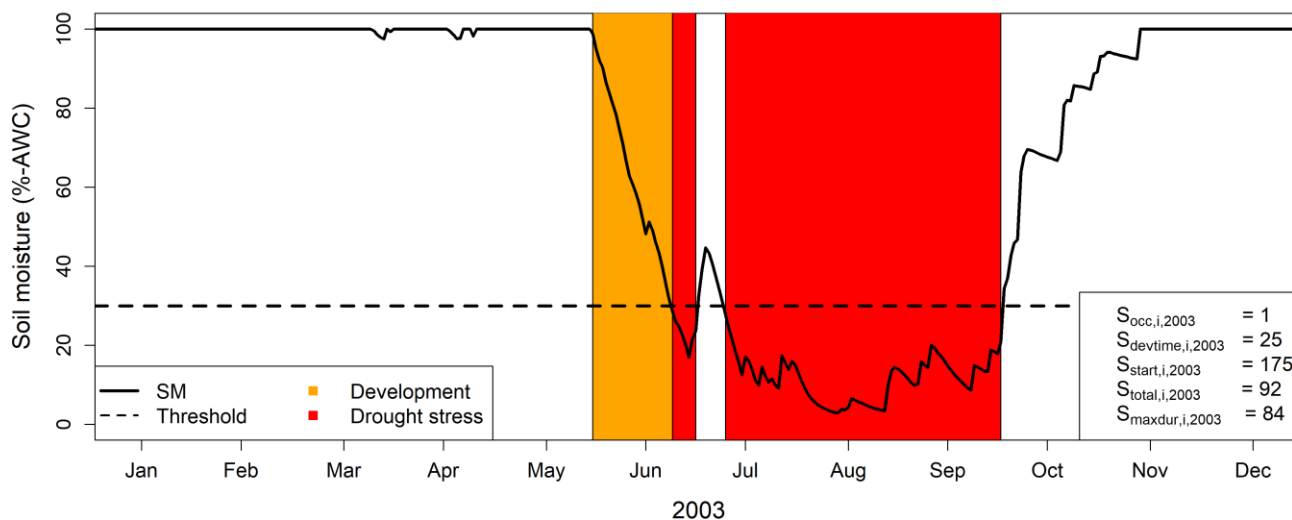
2.4 Soil moisture drought stress characteristics

We identified SM drought stress events, i.e., events where SM was continuously at or below a threshold (τ), from all daily simulated SM time series of agricultural grid cells. In this study, τ was set to 30% of the AWC (i.e., 30% of available water left in the root zone), which is in line with the threshold used by the German Weather Service to define possible drought stress (DWD, 2018). Various characteristics were calculated for the identified SM drought stress events. We first created a binary time series of SM drought stress occurrence (S_{occ}) for each agricultural grid cell ($i = 1, 2 \dots 15359$) and calendar year ($y = 1989, 1990 \dots 2018$), which indicates whether in a certain year or grid cell SM drought stress was reached ($S_{occ,i,y} = 1$) or not ($S_{occ,i,y} = 0$). Then, if $S_{occ,i,y} = 1$, various other SM drought stress characteristics were derived, namely:

175

$S_{start,i,y}$	The first day of SM drought stress (doy)
$S_{devtime,i,y}$	The development time of SM drought stress (days), i.e., the time it took to drop from field capacity (last day) to SM drought stress (first day).
$S_{total,i,y}$	The total time in SM drought stress (days), i.e., the number of days $SM_{i,y} < \tau$
$S_{maxdur,i,y}$	The maximum duration of SM drought stress (days), i.e., the maximum number of consecutive days with $SM_{i,y} < \tau$

These different SM drought stress characteristics are exemplified in Figure 3.



180 **Figure 3. Simulated soil moisture (SM) time series of an exemplary grid cell (i) showing the development and persistence of SM drought stress in 2003. The considered SM drought characteristics are presented in the lower-right legend, i.e., whether soil moisture drought stress developed or not ($S_{occ,i,2003}$) as well as the development time ($S_{devtime,i,2003}$), first day ($S_{start,i,2003}$), total number of days ($S_{total,i,2003}$) and maximum duration ($S_{maxdur,i,2003}$).**



2.5 Controls on SM drought stress characteristics

We related SM drought stress characteristics in different years (y) to the soil properties (AWC, Figure 1e) and climatological
185 setting (T_{annual} & P_{annual} , Figure 1b,c). Two different techniques were used:

- 1) Logistic regression for the binary data of $S_{\text{occ},y}$
- 2) Spearman's Rank correlation for the integer time series of $S_{\text{start},y}$, $S_{\text{devtime},y}$, $S_{\text{total},y}$ and $S_{\text{maxdur},y}$

190 Both the logistic regression and correlation analyses were carried out for each year separately to investigate whether the results were consistent over the years or exhibit a year-to-year variability.

2.6 Meteorological anomalies during (the development of) SM drought stress

We further characterized the meteorological anomalies during (the development of) SM drought stress. For all grid cells and years (and when $S_{\text{occ}}=1$), we calculated anomalies of P, T, and E (percentiles; resp. $P_{\text{perc},i,y}$, $T_{\text{perc},i,y}$, and $E_{\text{perc},i,y}$) during both
195 the development (dev) and annual maximum duration (maxdur) of SM drought stress. Weibull plotting positions were used to calculate these percentiles, i.e., $\text{rank}(x)/(n+1)$; where x is the meteorological variable of interest and n the sample size (in this study, $n=30$ years). The time window for which these percentiles were derived matches the time window of development and annual maximum duration. For the example in Figure 3, SM drought stress developed between the 31st of May and 24th of June and had its maximum duration between the 10th of July and 1st of October of 2003. For this event, $P_{\text{perc},\text{dev},i,2003}$,
200 $T_{\text{perc},\text{dev},i,2003}$ and $E_{\text{perc},\text{dev},i,2003}$ ($P_{\text{perc},\text{maxdur},i,2003}$, $T_{\text{perc},\text{maxdur},i,2003}$ and $E_{\text{perc},\text{maxdur},i,2003}$) express the meteorological anomalies of the period between the 31st of May and the 24th June (10th of July and 1st of October) in 2003, relative to the same time window in all other years.

For ease of notation, we omit the grid cell and year identifiers (i and y) from the variable subscripts in the remainder of this
205 paper.

3 Results

Figure 4 presents the percentage of grid cells that reached SM drought stress at least once in different calendar years ($S_{\text{occ}} = 1$). In general, results reveal a large temporal variability in the fraction of cells that reached SM drought stress. SM drought stress was reached in all years for at least a small proportion of the cells. However, most prominent drought years (i.e., the
210 years in which most cells reached SM drought stress) were 2003 and 2018, followed by 2015 and 1991. During these years, up to 89% of the grid cells reached SM drought stress.

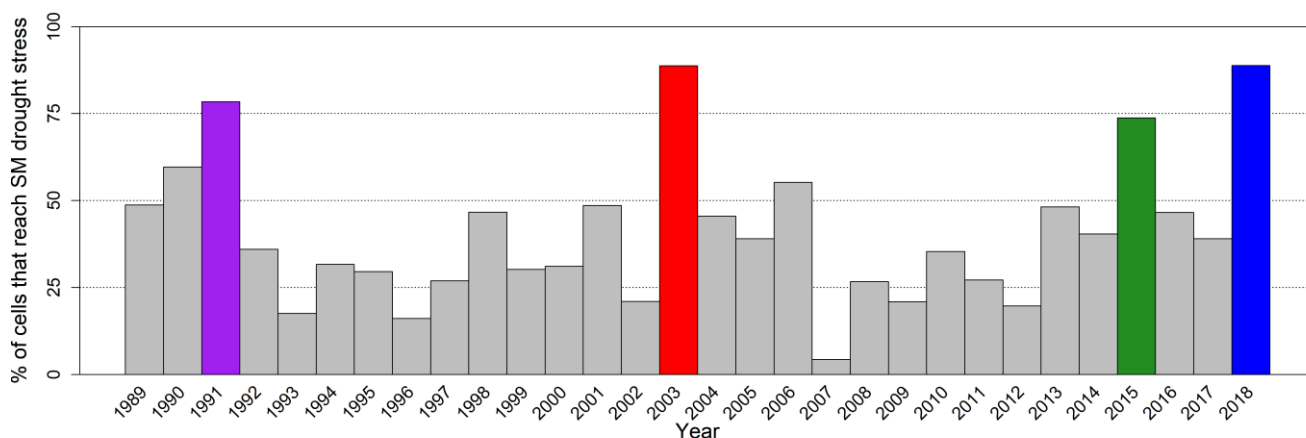
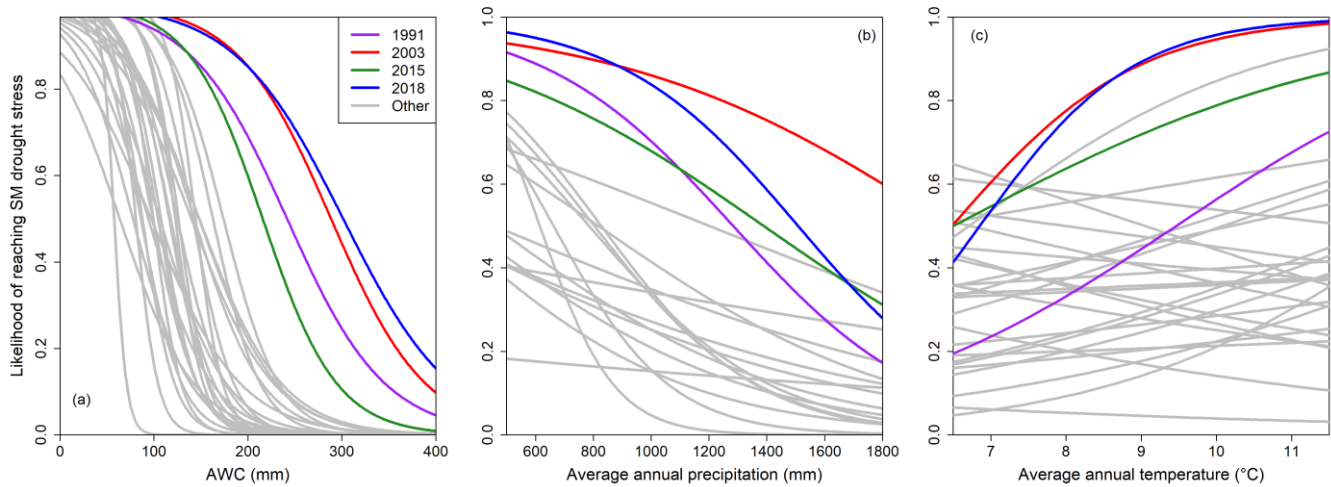


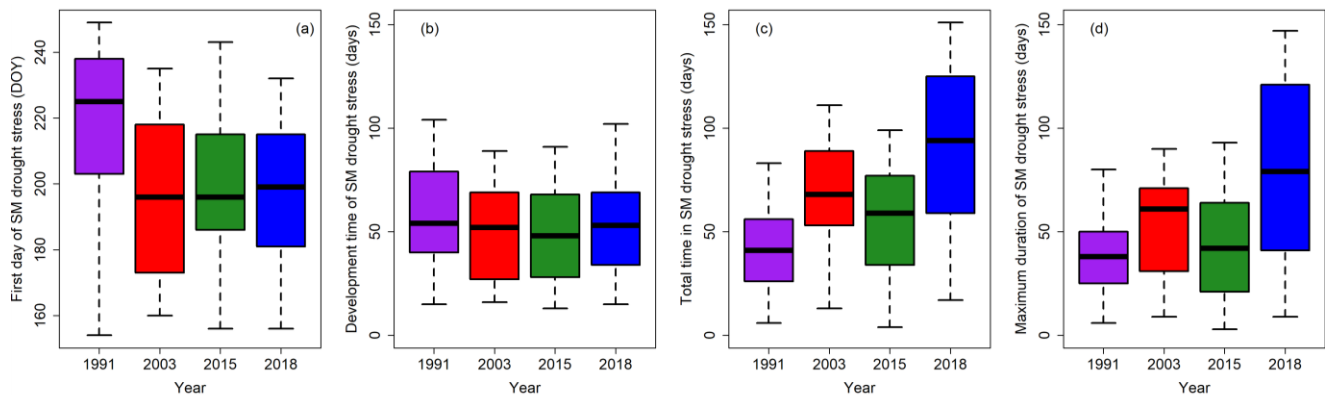
Figure 4. Percentage of cells that reached soil moisture drought stress for at least one day ($S_{occ} = 1$) in different calendar years. Most prominent years (1991, 2003, 2015 & 2018) are highlighted in colour.

215 Figure 5 shows the relationship between the likelihood of reaching SM drought stress (S_{occ}) and different controls (AWC, P_{annual} , T_{annual}). In general, likelihood functions derived with the AWC show a steeper and annually consistent increase than likelihood functions derived with P_{annual} and T_{annual} . The latter suggests a stronger influence of root zone soil characteristics, over the influence of the climatological setting, on whether or not SM drought stress developed. SM drought stress was further found to be more likely to develop in soils that have a lower AWC (Fig. 5a), as the likelihood of S_{occ} increases with decreasing AWC. The direction of increasing likelihood was consistent for every year, i.e., grid cells with a lower AWC
220 always had a higher likelihood of reaching SM drought stress than grid cells with a higher AWC. However, during the most prominent drought years, the likelihood functions are shifted to the right, revealing a higher likelihood of reaching SM drought stress for grid cells with a higher AWC during these dry years. SM drought stress was further found to be more likely to develop in drier regions with a lower P_{annual} (Fig. 5b). The likelihood of SM drought stress as a function of T_{annual}
225 shows more variation in the direction of increasing likelihood (Fig. 5c). In some years, including the prominent drought years, SM drought stress was more likely to develop in the warmer regions, but the latter was not the case for all considered years.



230 **Figure 5. Likelihood of reaching SM drought stress at least once in a year ($S_{occ} = 1$) as a function of (a) the AWC, (b) P_{annual} , (c) T_{annual} . Each curve reflects the likelihood function of a different year. Curves of prominent drought years are highlighted in colour.**

Figure 6 shows the variation in SM drought stress characteristics. In general, there was a lot of within year variability in these drought stress characteristics, whereas differences between prominent drought years were often less pronounced. S_{start} varies from the end of April to the end of September (Fig. 6a). The distribution of S_{start} is comparable between 2003, 2015 and 2018, whereas the distribution of S_{start} of 1991 indicates a generally later onset of SM drought stress. $S_{devtime}$ shows a large variability; from as little as 10 days up to around 4 months (Fig. 6b). Despite the large within year variability of $S_{devtime}$, there were no evident differences in the development time distribution among the prominent drought years. S_{total} shows both a large within year variability as well as distinct differences among the prominent drought years (Fig. 6c). The distribution of S_{total} reveals that 2003 and especially 2018 were characterized by the longest total time in SM drought stress (median $S_{total,2018} = 91$ days, 95th quantile $S_{total,2018} = 151$ days). A similar within year variability and between year differences was found for S_{maxdur} (Fig. 6d). Especially 2018 was characterized by persistent SM drought stress events (median $S_{maxdur,2018}$ of 79 days, 95th percentile of 147 days).





245 **Figure 6. Variability of different SM drought stress characteristics shown for the prominent drought years. Shown are (a) first day (S_{start}), (b) development time ($S_{devtime}$) (c) total number of days (S_{total}), and (d) maximum duration (S_{maxdur}) of SM drought stress. Box: percentiles 25, 50 and 75. End of whiskers: percentiles 5 and 95.**

Table 1 reveals Spearman’s rank correlation coefficient between various SM drought stress characteristics and the AWC of the root zone as well as the climatological setting (P_{annual} , T_{annual}) during prominent drought years. Both S_{start} and $S_{devtime}$ were most strongly correlated with the AWC, whereas the correlation with P_{annual} or T_{annual} was weaker or absent. These correlations imply that the start of soil moisture drought stress tends to be later and the development time tends to be longer for soils with a higher AWC. The correlations between the persistence of SM drought stress (S_{total} and S_{maxdur}) and the considered soil and climate controls suggest that the time in soil moisture drought stress tends to be longer for soils with a lower AWC that are located in drier and warmer domains of the study region. However, the correlations were weak or non-existent, and the sign of the correlation coefficient was not always consistent.

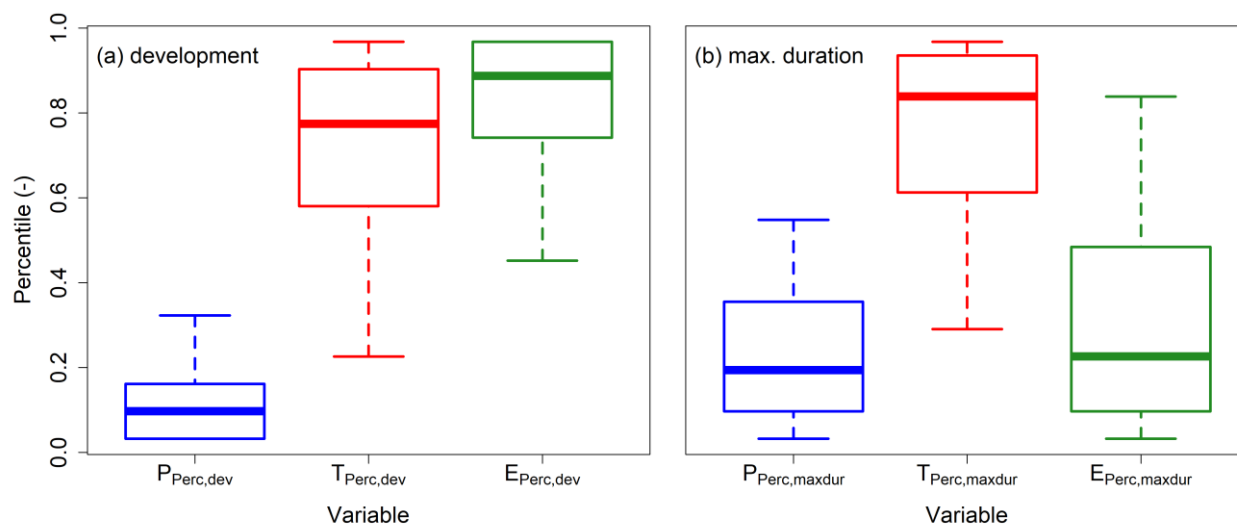
255 **Table 1. Spearman’s rank correlation coefficient between different SM drought stress characteristics; first day (S_{start}), development time ($S_{devtime}$), total time (S_{total}) and maximum duration (S_{maxdur}), and different soil and climate controls; available water-holding capacity of the root zone (AWC), annual average precipitation (P_{annual}) and annual average temperature (T_{annual}), during four prominent drought years.**

	Year	AWC	P_{annual}	T_{annual}
S_{start}	1991	0.72	0.15	0.02
	2003	0.71	0.08	-0.02
	2015	0.79	0.05	0.14
	2018	0.74	0.09	-0.04
$S_{devtime}$	1991	0.85	-0.34	0.48
	2003	0.77	-0.14	0.15
	2015	0.84	-0.37	0.53
	2018	0.77	-0.21	0.24
S_{total}	1991	-0.47	-0.35	0.14
	2003	-0.37	-0.37	0.31
	2015	-0.32	-0.22	0.12
	2018	0.09	-0.47	0.6
S_{maxdur}	1991	-0.38	-0.39	0.19
	2003	0.00	-0.46	0.44
	2015	-0.11	-0.21	0.24
	2018	0.23	-0.45	0.61

260 Figure 7 shows the meteorological anomalies during the development and annual maximum duration of SM drought stress (all events of all years combined). During the development of soil moisture drought stress, $P_{perc,dev}$ was almost always anomalously low, whereas $T_{perc,dev}$ and especially $E_{perc,dev}$ were often anomalously high (Fig. 7a). The distribution of $E_{perc,dev}$ and especially $T_{perc,dev}$ shows a larger spread than the distribution of $P_{perc,dev}$. The latter implies that especially P needed to be anomalously low for SM drought stress to develop, whereas E and T could be more variable during the development. During the annual maximum duration SM drought stress event, $P_{perc,maxdur}$ was again generally anomalously low (Fig. 7b). However,



265 $P_{\text{perc,maxdur}}$ shows a larger variation and spread and was generally higher than $P_{\text{perc,dev}}$. $T_{\text{perc,maxdur}}$ and $E_{\text{perc,maxdur}}$ show contrasting anomalies, where T was often above normal and E often below normal during the annual maximum duration SM drought stress event.



270 **Figure 7. Meteorological anomalies (percentiles) of precipitation (P_{perc}), temperature (T_{perc}) and actual evapotranspiration (E_{perc}) during (a) the development (dev) and (b) the annual maximum duration (maxdur) of SM drought stress. Box: percentiles 25, 50 and 75. End of whiskers: percentiles 5 and 95.**

4 Discussion

Our first objective was to characterize the occurrence, development time and persistence of simulated past soil moisture (SM) drought stress events. Results revealed a large temporal variability in the amount of grid cells that reach SM drought stress in a certain year (Figure 4). The most extreme SM drought stress years were 2003 and 2018, during which up to 89 percent of the agricultural grid cells reached SM drought stress. Previous studies already showed that 2003 was an extreme drought year within and around the study region (e.g., Ionita et al., 2016). Results of this study imply that the recent 2018 event was comparable to 2003 in terms of the amount of grid cells that reach SM drought stress. However, even during more severe drought years, simulated SM drought stress did not develop for some of the agricultural grid cells, either because of 1) local variations in meteorological conditions (e.g. local rains storms) and 2) root zone soils having a large enough storage capacity that acted as a buffer during dry conditions. This illustrates that even during the most extreme drought years, regional differences can occur. The factors that control these differences, i.e., the occurrence of local rainstorms and differences in soil characteristics can be spatially heterogeneous. The latter implies that regional agricultural drought assessments should occur at a relatively high spatial resolution to be able to capture these differences.

285 A large variability in the development time of simulated SM drought stress was found (Fig. 6b). SM drought stress could develop in less than 10 days, e.g., in shallow root zones with a low available water holding capacity (AWC). This is faster



than the minimum development time of 30 days used to identify rapid-onset (flash) droughts in, e.g., Christian et al., 2019. On the other hand, it could also take a lot longer (up to 4 months) for SM drought stress to develop. This slower development matches better with the traditional description of drought, being a slowly developing (creeping) phenomena (Wilhite & Glantz, 1985). Overall, the large differences in development time suggest that different types of forecasting systems could be suitable to predict the development of agricultural drought; medium range weather forecasts for quickly developing events and more long-term meteorological forecasts for slower developing episodes.

The persistence of SM drought stress (total days and maximum duration) varied strongly between years and grid cells (Fig. 5c,d). Results of this study showed that the total days and maximum duration of SM drought stress was generally highest in 2018, making this event more severe than earlier (recent) benchmark events, such as 2003. The long nature of the drought of 2018 was also found in a recent study for Switzerland, the country directly south of our study region, in Brunner et al., (2019). We also found that the annual maximum duration and total time of SM drought stress never exceeded 6 months, and most of the root zones reached field capacity again each year before the start of the new growing season. Thus, SM drought stress was never a multi-year phenomenon for the considered agricultural grid cells.

Our second objective was to investigate the dominant controls on the likelihood, development time and persistence of SM drought stress. Both likelihood and development time were most strongly related to the AWC of the root zone and less to the climatological setting (Fig. 5, Table 1). SM drought stress was generally more likely to develop, and evolved faster and earlier in the year, in shallow root zones with a lower AWC. These findings are in line with results for the 2012 flash drought in the US presented by Otkin et al. (2016), where anomalous soil moisture conditions generally first appeared in the topsoil layer (lower AWC) and only later in the entire soil layer (higher AWC). Results also confirm that AWC of the root zone is an important factor to determine the vulnerability to agricultural drought, as was also stated in, e.g., Wilhelmi & Wilhite (2004). Finally, these results imply that agricultural drought assessments purely based on meteorological proxy indicators should be interpreted with care, as they might not consider differences in root zone soil characteristics.

The persistence of SM drought stress was only weakly correlated with the AWC of the root zone and climatological setting (Table 1). The reason for overall weaker correlations might be related to the different mechanisms that govern the persistence of SM drought stress in different types of root zones. In root zones with a low AWC, SM drought stress can develop rather quickly. However, the total deficit that can build up is limited and only a small rainfall event is enough to alleviate SM drought stress conditions. In root zones with a high AWC, larger SM deficits can potentially develop. However, this development takes longer, and the SM drought stress threshold is only exceeded towards the end of the growing season, after which further development is limited because of lacking evapotranspiration. The most persistent SM drought stress events might therefore occur for root zones with an intermediate AWC. In these root zones, SM drought stress can develop reasonably fast but can also build up a large enough deficit that can endure some smaller rainfall events.

The third objective of this study was to portray the meteorological anomalies during (the development of) simulated SM drought stress. During the development, especially precipitation needed to be anomalously low (Fig. 7a), suggesting that lacking precipitation was the most important prerequisite for SM drought stress to develop. However, also air temperature



and especially evapotranspiration were often above normally high during the development of SM drought stress, implying an enhancing (compound) effect of these variables (see also Manning et al., 2018). During the annual maximum duration SM drought stress events, precipitation was often below normal as well (Fig. 7b). However, precipitation anomalies during the maximum duration events were not as extreme as during the development, possibly because SM only needed to remain in a steady state condition of SM drought stress rather than having to decline from field capacity to a level of SM drought stress. Temperature and simulated evapotranspiration show contrasting anomalies during the annual maximum duration SM drought stress events, with temperature generally being above- and simulated evapotranspiration generally being below-normal. The reason for these contrasting anomalies might be related to a different energy partitioning of heat fluxes during SM drought stress (described in e.g., Seneviratne et al., 2010). During SM drought stress, simulated evapotranspiration was anomalously low because of the vegetative stress assumed in the model that causes plants to limit their evapotranspiration. The incoming solar radiation that is normally consumed by evapotranspiration (latent heat flux) is now used to warm up the soil and lower atmosphere (sensible heat flux), possibly explaining the above normal temperatures during SM drought stress (Miralles et al., 2014). This energy partitioning during SM drought stress and resulting contrasting temperature and evapotranspiration anomalies highlight that agricultural drought assessments derived from (temperature-based) meteorological proxy indicators based on potential evapotranspiration should be interpreted with care.

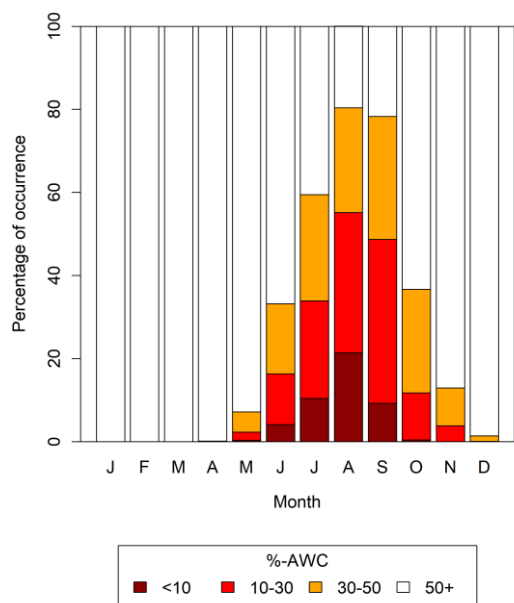
Our regional assessment of SM drought stress is subject to inaccuracies, challenges, and assumptions; something common for these kinds of analyses. One source of inaccuracies relates to the modeling of SM. Previous studies showed that the physical based TRAIN model was able to provide a good temporal representation of soil moisture over agricultural fields (e.g., Stork & Menzel, 2016). However, it is important to bear in mind that the studied results are regional model simulations for a specific soil and general land use parameterizations that can differentiate from the heterogeneous real world. In addition, there are other models, model structures and model parameterizations to simulate soil moisture, implying a dependency between the used model (parameterization) and the results (shown in e.g., Samaniego et al., 2018; Zink et al., 2017). The latter studies use ensembles of resp. different models or different model parameterizations to consider model or parameter related uncertainties; something outside the scope of the current study.

Another source of inaccuracies stems from the data used to set-up and force the model. One challenge was the interpolation of several different meteorological variables over a rather complex terrain, which is prone to biases. Another challenge was the spatially accurate representation of the root zone soil, both in terms of the interpolation of heterogeneous soil and land use characteristics as well as in the parameterization of the rooting depth. The interpolation of soil and land use characteristics was based on the majority class within a 1-km grid cell. However, each grid cell can still exhibit a large variability in soil and land use characteristics, implying that the simulated SM dynamics might not be representative for the entire grid cell. The parameterization of the rooting depth of each grid cell was further based on soil characteristics, which is a more often used procedure to parameterize regional models. However, roots do not necessarily utilize the water in the entire soil column, and rooting depth is depending on other factors such as the type of crop. For example, a soil might have a maximum rooting depth of a meter; however, if a shallow rooting crop species is grown on this soil, roots may not have



355 access to all water. Overall, the soil-based parametrization of the root zone as well as the possible variability of soil and land
use characteristics within a grid cell means that results might not always be accurate for a specific grid cell or for a single
agricultural field located within this grid cell. However, by analyzing a large sample of grid cells, we cover most
combinations of root zone characteristics and climatological settings that occur within the study region (Fig. 1). Lessons
learned from this large sample, e.g., about the relationship between SM drought stress characteristics and soil properties (e.g.
360 Fig. 5, Table 1), are therefore likely to be applicable at the smaller (local) scales within the study region.

An assumption that was made in this study relates to the definition of SM drought. In this study, we defined SM drought in
an absolute way rather than as an anomaly. We used one fixed threshold of 30% of the AWC to define SM drought stress.
This threshold is in line with the indicative threshold for SM drought stress used by e.g. the German Weather Service (DWD,
2018). However, it should be noted that this threshold, as well as the relationship between the degree of SM drought stress
365 and the amount of available water left in the root zone, varies depending on, e.g., crop species, crop development stage,
climatological conditions and soil type (Allen et al., 1998). Notwithstanding these assumptions, we believe that from an
agricultural drought impact perspective, an absolute definition of SM drought stress could be more closely related to actual
water stress experienced by plants than an anomaly-based definition. Especially so because soil moisture anomalies can be
significantly different from a low water availability in the root zone, in particular during the non-growing season, as is
370 shown for the considered agricultural grid cells in Figure 8. The proposed absolute definition of SM drought stress might be
applicable in other regions or for other drought research purposes, e.g., that aim to investigate changes in agricultural
drought under climate change.



375 **Figure 8. Distribution of daily soil moisture values (expressed as % of the available water-holding capacity left in the root zone) during anomalously low soil moisture conditions (daily SM percentile < 0.25) shown for all agricultural grid cells grouped by calendar month.**



5 Conclusion

Meteorological droughts cause soil moisture levels to decline. Diminished root zone soil moisture can largely affect agricultural productivity, as crops might experience soil moisture drought stress. In this study, we investigated the characteristics of simulated past soil moisture drought stress events across Southwestern Germany as well as their relationship with different soil and climate variables. The total agricultural area that reached soil moisture drought stress conditions was found to vary strongly among the years and was highest in 2003 and 2018. In terms of the development time, 2003 was not much different from 2018. In both years, development time varied from as little as 10 days to up to four months. What made 2018 distinctively different from 2003 was the generally longer total time and maximum duration of simulated soil moisture drought stress, highlighting the extraordinary severity of the most recent event studied. Both the occurrence and development time of soil moisture drought stress were found to be strongly related to the available water-holding capacity of the root zone and not so much to the climatological setting. This stresses the importance of considering differences in root zone storage characteristics for agricultural drought assessments. Results of this study further imply that below normal precipitation was the most important reason for soil moisture drought stress to develop. However, the often above normal anomalies of temperature and especially simulated evapotranspiration during development, suggest an augmenting effect of these variables. During simulated soil moisture drought stress, temperature anomalies were found to be often above normal, which contradicted with the often below normal simulated evapotranspiration anomalies. These contrasting anomalies of temperature and evapotranspiration imply that agricultural drought assessments derived from meteorological proxies based on potential evapotranspiration should be interpreted with care. The same is the case for agricultural assessments based on soil moisture anomalies, as below normal anomalies were found to not necessarily correspond to a situation of soil moisture drought stress. The in this study presented approach of directly characterizing simulated soil moisture drought stress events for agricultural drought assessments might in some cases be a suitable alternative to approaches based on soil moisture anomalies.

Code and data availability. Gridded model simulations of soil moisture used in this study as well as animations of the latter during major drought events are available from the Heidata repository of the Heidelberg University. The following DOI is reserved and will become active upon acceptance <https://doi.org/10.11588/data/PRXZAS>. For reviewing purposes, the data is accessible via the following link <https://heidata.uni-heidelberg.de/privateurl.xhtml?token=fb658f7f-0ec8-49db-84d0-a8e726936743>). Input data for the model can be derived from publicly available sources (Section 2.2). The plot version of the TRAIN model and R-code used to analyze the simulations and visualize the results can be requested from the authors.

Author contributions. ET and LM designed the study. ET prepared the data, carried out the analyses, wrote the manuscript and prepared the Figures and Table. LM provided input on the analyses and edited the paper.



410 **Competing interests.** The authors declare that they do not have competing interests.

Acknowledgements. This work contributes to the DRIeR project supported by the Wassernetzwerk Baden-Württemberg (Water Research Network), which is funded by the Ministerium für Wissenschaft, Forschung und Kunst Baden-Württemberg (Ministry of Science, Research and the Arts of the State Baden-Wuerttemberg). We thankfully acknowledge Verena Maurer
415 for her help with interpolating the soil and land cover grids, Anna Buch for testing and preparing the SARAH global radiation data as TRAIN input and Nicole Gerlach for her help with the INTERMET Software. We further acknowledge all agencies that provided the data used for the simulations, specifically the Federal Agency for Cartography and Geodesy (BKG), the German Environment Agency (UBA), the Federal State Office for Geology Resources and Mining (LGRB), the German Weather Service (DWD) and the Satellite Application Facility on Climate Monitoring (CM SAF). All analyses were
420 carried out with the open-source software R (<https://www.r-project.org/>), partially using the packages “raster”, “rgdal” and “rdwd”.

References

- Allen, R. G., Pereira, L. S., Raes, D. and Smith, M.: Crop Evapotranspiration – Guidelines for computing crop water requirements, FAO Irrigation and Drainage Paper 56, FAO, Rome, Italy, 1998.
- 425 Andreadis, K. M., Clark, E. A., Wood, A. W., Hamlet, A. F. and Lettenmaier, D. P.: Twentieth-century drought in the conterminous United States, *J. Hydrometeorol.*, 6, 985–1001, <https://doi.org/10.1175/JHM450.1>, 2005.
- Berg, A. and Sheffield, J.: Climate Change and Drought: the Soil Moisture Perspective, *Current Climate Change Reports*, 4, 180–191. <https://doi.org/10.1007/s40641-018-0095-0>, 2018.
- Bergstrom, S.: The HBV model, in: *Computer Models of Watershed Hydrology*, edited by: Singh, V. P., Water Resources
430 Publications: Highlands Ranch, Colorado, USA, 1995.
- BKG (Federal Agency for Cartography and Geodesy): Digital Elevation Model 1000 m (DGM1000), retrieved from <http://www.geodatenzentrum.de> in 2018.
- Brunner, M. I., Liechti, K. and Zappa, M.: Extremeness of recent drought events in Switzerland: dependence on variable and return period choice, *Nat. Hazards Earth Syst. Sci.*, 19, 2311–2323, <https://doi.org/10.5194/nhess-19-2311-2019>, 2019.
- 435 Christian, J. I., Basara, J. B., Otkin, J. A., Hunt, E. D., Wakefield, R. A., Flanagan, P. X. and Xiao, X.: A Methodology for Flash Drought Identification: Application of Flash Drought Frequency across the United States, *J. Hydrometeorol.*, 20, 833–846, <https://doi.org/10.1175/jhm-d-18-0198.1>, 2019.
- Dobler, L., Gerlach, N. and Hinterding, A.: INTERMET - Interpolation stündlicher und tagesbasierter meteorologischer Parameter, Federal state office for the environment of Rhineland Palatinate, Mainz, Germany, 2004 (in German).
- 440 DWD (German Weather Service): Dokumentation Bodenfeuchte, German Weather Service (DWD), Offenbach, Germany, 2018 (in German).



- DWD (German Weather Service): Climate Data Center; used are grids and observation for Germany, Retrieved from ftp://opendata.dwd.de/climate_environment/CDC/ in 2019
- Hanel, M., Rakovec, O., Markonis, Y., Máca, P., Samaniego, L., Kyselý, J. and Kumar, R.: Revisiting the recent European
445 droughts from a long-term perspective, *Sci. Rep.*, 8, 1–11, <https://doi.org/10.1038/s41598-018-27464-4>, 2018.
- Hunt, E. D., Hubbard, K. G., Wilhite, D. A., Arkebauer, T. J. and Dutcher, A. L.: The development and evaluation of a soil
moisture index, *Int. J. Climatol.*, 29, 747-759, <https://doi.org/10.1002/joc.1749>, 2009.
- LGRB (Federal State Office for Geology Resources and Mining): Soil maps for Baden-Württemberg (BK50), retrieved
from <https://lgrb-bw.de/bodenkunde> in 2018
- 450 Lloyd-Hughes, B.: The impracticality of a universal drought definition, *Theor. Appl. Climatol.*, 117, 607–611,
<https://doi.org/10.1007/s00704-013-1025-7>, 2014.
- Manning, C., Widmann, M., Bevacqua, E., Van Loon, A. F., Maraun, D. and Vrac, M.: Soil Moisture Drought in Europe: A
Compound Event of Precipitation and Potential Evapotranspiration on Multiple Time Scales. *J. Hydrometeorol.*, 19, 1255–
1271. <https://doi.org/10.1175/jhm-d-18-0017.1>, 2018.
- 455 Menzel, L.: Modelling canopy resistances and transpiration of grassland. *Phys. Chem. Earth*, 21, 123-129,
[https://doi.org/10.1016/S0079-1946\(97\)85572-3](https://doi.org/10.1016/S0079-1946(97)85572-3), 1996.
- Menzel, L.: Modellierung der Evapotranspiration im System Boden-Pflanze-Atmosphäre, *Zür. Geogr. Schr.*, 67, Institute of
Geography, ETH Zürich, Zürich, Switzerland, 1997 (in german).
- Miralles, D. G., Teuling, A. J., van Heerwarden, C. C. and Vilá-Guerau de Arellano, J.: Mega heatwave temperatures due to
460 combined soil desiccation and atmospheric heat accumulation, *Nature Geosci.*, 7, 345–349,
<https://doi.org/10.1038/ngeo2141>, 2014.
- Otkin, J. A., Anderson, M. C., Hain, C., Mladenova, I. E., Basara, J. B. and Svoboda, M.: Examining Rapid Onset Drought
Development Using the Thermal Infrared–Based Evaporative Stress Index, *J. Hydrometeorol.*, 14, 1057-1074,
<https://doi.org/10.1175/jhm-d-12-0144.1>, 2013.
- 465 Otkin, J. A., Anderson, M. C., Hain, C., Svoboda, M., Johnson, D., Mueller, R., Tadesse, T., Wardlow, B. and Brown, J.:
Assessing the evolution of soil moisture and vegetation conditions during the 2012 United States flash drought, 218, 230-
242, *Agr. Forest Meteorol.*, <https://doi.org/10.1016/j.agrformet.2015.12.065>, 2016.
- Otkin, J. A., Svoboda, M., Hunt, E. D., Ford, T. W., Anderson, M. C., Hain, C. and Basara, J. B.: Flash droughts: A review
and assessment of the challenges imposed by rapid-onset droughts in the United States, *B. Am. Meteorol. Soc.*, 99, 911-919,
470 <https://doi.org/10.1175/BAMS-D-17-0149.1>, 2018.
- Palmer, W. C.: Meteorological Drought, Tech. Rep. 45, US Department of Commerce, Weather Bureau, Washington D.C.,
USA, 1965.
- Pfeifroth, U., Kothe, S., Trentmann, J., Hollmann, R., Fuchs, P., Kaiser, J. and Werscheck, M.: Surface Radiation Data Set -
Heliosat (SARAH) - Edition 2.1, Satellite Application Facility on Climate Monitoring,
475 https://doi.org/10.5676/EUM_SAF_CM/SARAH/V002_01, 2019a.



- Pfeifroth, U., Trentmann, J., Hollmann, R., Selbach, N., Werscheck, M. and Meirink, J. F.: ICDR SEVIRI Radiation - based on SARAH-2 methods, Satellite Application Facility on Climate Monitoring, retrieved from https://wui.cmsaf.eu/safira/action/viewICDRDetails?acronym=SARAH_V002_ICDR, 2019b.
- 480 Rauthe, M., Steiner, H., Riediger, U., Mazurkiewicz, A. and Gratzki, A.: A Central European precipitation climatology - Part I: Generation and validation of a high-resolution gridded daily data set (HYRAS). *Meteorol. Z.*, 22, 235–256, <https://doi.org/10.1127/0941-2948/2013/0436>, 2013.
- Samaniego, L., Kumar, R. and Attinger, S.: Multiscale parameter regionalization of a grid-based hydrologic model at the mesoscale, *Water Resour. Res.*, 46, <https://doi.org/10.1029/2008WR007327>, 2010.
- 485 Samaniego, L., Kumar, R. and Zink, M.: Implications of Parameter Uncertainty on Soil Moisture Drought Analysis in Germany. *J. Hydrometeorol.*, 14, 47–68. <https://doi.org/10.1175/jhm-d-12-075.1>, 2012.
- Samaniego, L., Thober, S., Kumar, R., Wanders, N., Rakovec, O., Pan, M., Zink, M., Sheffield, J., Wood, E. F. and Marx, A.: Anthropogenic warming exacerbates European soil moisture droughts, *Nat. Clim. Change*, 8, 421–426, <https://doi.org/10.1038/s41558-018-0138-5>, 2018.
- 490 Seneviratne, S. I., Corti, T., Davin, E. L., Hirschi, M., Jaeger, E. B., Lehner, I., Orlowsky, B. and Teuling, A. J.: Investigating soil moisture-climate interactions in a changing climate: A review, *Earth-Sci. Rev.*, 99, 125–161, <https://doi.org/10.1016/j.earscirev.2010.02.004>, 2010.
- Sheffield, J., Goteti, G., Wen, F. and Wood, E. F.: A simulated soil moisture based drought analysis for the United States, *J. Geophys. Res-Atmos.*, 109, 1–19. <https://doi.org/10.1029/2004JD005182>, 2004.
- 495 Sheffield, J. and Wood, E. F.: Characteristics of global and regional drought, 1950–2000: Analysis of soil moisture data from off-line simulation of the terrestrial hydrologic cycle, *J. Geophys. Res-Atmos.*, 112, <https://doi.org/10.1029/2006JD008288>, 2007.
- Sheffield, J., Wood, E. F. and Roderick, M. L.: Little change in global drought over the past 60 years, *Nature*, 491, 435–438. <https://doi.org/10.1038/nature11575>, 2012.
- 500 Stahl, K., Kohn, I., Blauhut, V., Urquijo, J., De Stefano, L., Acácio, V., Dias, S., Stagge, J. H., Tallaksen, L. M., Kampragou, E., Van Loon, A. F., Barker, L. J., Melsen, L. A., Bifulco, C., Musolino, D., de Carli, A., Massarutto, A., Assimacopoulos, D., and Van Lanen, H. A. J.: Impacts of European drought events: insights from an international database of text-based reports, *Nat. Hazards Earth Syst. Sci.*, 16, 801–819, <https://doi.org/10.5194/nhess-16-801-2016>, 2016.
- Stork, M. and Menzel, L.: Analysis and simulation of the water and energy balance of intense agriculture in the Upper Rhine valley, south-west Germany, *Environ. Earth Sci.*, 75, <https://doi.org/10.1007/s12665-016-5980-z>, 2016.
- 505 Svoboda, M., LeComte, D., Hayes, M., Heim, R., Gleason, K., Angel, J., Rippey, B., Tinker, R., Palecki, M., Stooksbury, D., Miskus, D. and Stephens, S.: The drought monitor, *B. Am. Meteorol. Soc.*, 83, 1181–1190. [https://doi.org/10.1175/1520-0477\(2002\)083<1181:TDM>2.3.CO;2](https://doi.org/10.1175/1520-0477(2002)083<1181:TDM>2.3.CO;2), 2002.
- Törnros, T. and Menzel, L.: Addressing drought conditions under current and future climates in the Jordan River region, *Hydrol. Earth Syst. Sci.*, 18, 305–318, <https://doi.org/10.5194/hess-18-305-2014>, 2014.



- 510 UBA (German Environment Agency): CORINE Land Cover Germany 25 ha – 2006, retrieved from <https://gis.uba.de/catalog/Start.do> in 2018.
- UN/ISDR: Drought Risk Reduction Framework and Practices: contributing to the implementation of the Hyogo Framework for Action, United Nations Secretariat of the International Strategy for Disaster Reduction (UNISDR), Geneva, Switzerland, 2009.
- 515 Vicente-Serrano, S. M., Beguería, S. and López-Moreno, J. I.: A multiscalar drought index sensitive to global warming: The standardized precipitation evapotranspiration index, *J. Climate*, 23, 1696–1718, <https://doi.org/10.1175/2009JCLI2909.1>, 2010.
- Wang, A., Lettenmaier, D. P. and Sheffield, J.: Soil moisture drought in China, 1950-2006, *J. Climate*, 24, 3257–3271. <https://doi.org/10.1175/2011JCLI3733.1>, 2011.
- 520 Wilhelmi, O. V. and Wilhite, D. A.: Methodology for assessing vulnerability to agricultural drought: a Nebraska case study, *Nat. Hazards*, 25, 37–58, 2002.
- Wilhite, D. A. and Glantz, M. H.: Understanding the Drought Phenomenon: The Role of Definitions, *Water Int.*, 10, 111–120. <https://doi.org/10.1080/02508068508686328>, 1985.
- Zink, M., Kumar, R., Cuntz, M. and Samaniego, L.: A high-resolution dataset of water fluxes and states for Germany accounting for parametric uncertainty, *Hydrol. Earth Syst. Sci.*, 21, 1769–1790, <https://doi.org/10.5194/hess-21-1769-2017>, 2017.
- 525 Zink, M., Samaniego, L., Kumar, R., Thober, S., Mai, J., Schafer, D. and Marx, A.: The German drought monitor, *Environ. Res. Lett.*, 11, <https://doi.org/10.1088/1748-9326/11/7/074002>, 2016.